[American Journal of Science, Vol. 310, April, 2010, P. 261–281, DOI 10.2475/04.2010.02]

THERMOTECTONIC EVIDENCE FOR TWO-STAGE EXTENSION ON THE TRINITY DETACHMENT SURFACE, EASTERN KLAMATH MOUNTAINS, CALIFORNIA

GEOFFREY E. BATT*, SUSAN M. CASHMAN**, JOHN I. GARVER***, and JEFFREY J. BIGELOW§,§§

ABSTRACT. We present integrated fission-track and (U-Th)/He analysis of a reconnaissance suite of 8 apatite samples along a transect crossing the footwall of the Trinity Detachment Surface, a variably preserved low-angle extensional structure in the Eastern Klamath Mountains of California. These thermochronological data display significant variation when plotted along the extension lineation evident on exposed remnants of the fault, and the combined ages, together with the fission track length variation observed, require two discrete episodes of exhumation associated with extension on this structure. Consistent mid-Cretaceous fission-track ages indicate continuation of earlier slip on the detachment surface and/or erosional exhumation to bring upper greenschist facies footwall rocks into the brittle upper crustal domain. This phase of exhumation continued until c. 80 Ma, terminating while currently exposed samples were still 2 to 3 km below the surface. Final exhumation of the footwall block occurred in a second discrete episode initiating at c. 20 to 23 Ma, contemporaneous with development or re-activation of extension on the La Grange Fault to the south.

Key words: Klamath Mountains, Thermochronology, Fission track, (U-Th)/He, Tectonics.

INTRODUCTION

The Klamath Province of northern California and southern Oregon formed through Devonian-Jurassic accretion of oceanic terranes and Jurassic-Cretaceous calc-alkaline magmatism (Irwin, 1972, 2003; Snoke and Barnes, 2006; Ernst and others, 2008) at a long-lived convergent plate boundary. Although much of this geological history is shared with rocks of the Sierra Nevada foothills (Irwin, 2003; Ernst and others, 2008), a number of distinctive features suggest that the Cenozoic history of the Klamath Province merits further examination.

The Klamath Mountains represent the highest terrain in the coastal ranges of the Cascadia forearc, with an average topographic height three times that of the Oregon Coast Range to the north (Kelsey and others, 1994; Brudzinski and Allen, 2007). This striking topographic signature is also underlain by the oldest rocks (Lindsley-Griffin and others, 2006) and the only demonstrable evidence of late Cenozoic detachment faulting within the Cascadia forearc system (Schweickert and Irwin, 1989). Rocks and surfaces in the Klamath Mountains locally record substantial recent surface uplift (Diller, 1902; Aalto, 2006) and rock uplift (Mortimer and Coleman, 1985). Information on the timing and distribution of bedrock uplift in the Klamath Mountains Province is required before the tectonic processes driving the Cenozoic development of this region can be understood.

* John de Laeter Centre of Mass Spectrometry, School of Earth and Environment, The University of Western Australia, Crawley, WA 6009, Australia; gbatt@cyllene.uwa.edu.au
** Department of Geology, Humboldt State University, Arcata, California 95521, USA
*** Department of Geology, Union College, 807 Union St., Schenectady, New York, 12308-2311, USA
§ Delta Environmental Consultants Inc., 2065 Sidewinder Dr., Park City, Utah 84060
§§ Formerly at Department of Geology, Union College, 807 Union St., Schenectady, New York 12308-2311, USA

A potentially significant record of uplift and exhumation is preserved by a group of low-angle detachment faults in the southeastern Klamath Mountains, their uplifted footwall (the "Trinity Arch" of Irwin and Lipman, 1962), and several small hanging wall basins containing Upper Cretaceous and/or Cenozoic sedimentary fill (Weaverville Basin, and the Lowden Ranch and Reading Creek Grabens). Cenozoic detachment faulting was initially recognized by Schweickert and Irwin (1989) at the La Grange Mine, where hydraulic mining of gold-bearing gravels has exposed a 1-km-long segment of the fault surface. At this locality, mid-Tertiary Weaverville Formation sediments in the hanging wall of the fault dip shallowly (~10°) northwest toward the shallowly southeast-dipping fault surface (MacDonald, 1910). Subsequent mapping of discontinuous fault segments and hanging wall klippen in the surrounding region has delineated a group of faults that share a common early history as a unified detachment structure—here referred to as the Trinity Detachment Surface—but provide incomplete and locally conflicting evidence for the timing and extent of faulting during at least two deformation episodes (Cashman and Elder, 2002; Fudge, ms, 2008).

Extensive field evidence for the kinematic history of this detachment surface was presented by Cashman and Elder (2002). We here follow this work, assessing uplift and exhumation around the structure through application of low-temperature thermochronometry to a reconnaissance suite of samples from Early Cretaceous plutons exposed in its footwall (fig. 1). Combined with stratigraphic (Phillips and Aalto, 1989) and palynological (Barnett, 1989) investigations of hanging wall rocks, the sensitivity of our apatite fission-track and (U-Th)/He analyses to denudation provides significant new constraint on both the timing and magnitude of exhumation on the Trinity Detachment Surface, and clarifies the Cenozoic uplift history of the Klamath Mountains.

GEOLOGICAL SETTING

The Klamath Mountains consist of a structurally imbricated stack of east-dipping and generally westward-younging terranes, separated by thrust faults (for example, Evernden and Kistler, 1970; Irwin, 1985; Irwin and Mankinen, 1998; Irwin and Wooden, 1999) (fig. 1). From Devonian to mid-Jurassic time, evolution of the province proceeded by the sequential accretion of ophiolite-chert-argillite terranes (Irwin, 1972; Davis and others, 1979; Irwin and Wooden, 1999; Ernst and others, 2008). This accretionary phase terminated with the Late Jurassic Nevadan orogeny, which produced regional deformation, metamorphism, and the development of a slaty cleavage (for example, Davis and others, 1965; Lanphere and others, 1968; Saleeby and others, 1982; Irwin, 1985; Cashman, 1988; Harper and others, 1994; Ernst and others, 2008).

Subduction along the western margin of North America during the Early Cretaceous resulted in substantial calc-alkaline igneous activity within the Klamaths (Ernst and others, 2008). In the east-central Klamath Mountains, a distinctive suite of low-K plutons, the tonalite-trondhjemite-granodiorite suite (ttg suite) of Barnes and others (1996), was emplaced over a short period between ~142 Ma (Deadman Peak pluton) and ~136 Ma (Craggy Peak and Sugar Pine plutons) (Barnes and others, 1996; Irwin and Wooden, 1999; Allen and Barnes, 2006).

These plutons lie structurally below the Trinity Detachment Surface, and provide a useful baseline for assessing footwall uplift and exhumation because of their restricted age range and well-documented crystallization conditions. Magmatic temperatures for the ttg suite range between 940 and 820°C, with mean values of 907 ± 21°C for the Deadman Peak and 880 ± 23°C for the Craggy Peak plutons sampled in this study (Barnes and others, 1996). Corresponding emplacement pressures are estimated at 2±1 kbar based on contact metamorphic assemblages (Goodge, 1989), and at 2.5 to 3.5 kbar based on aluminium-in-hornblende barometry (Barnes and others, 1996), yielding an estimated emplacement depth of ~ 7 to 10 km.

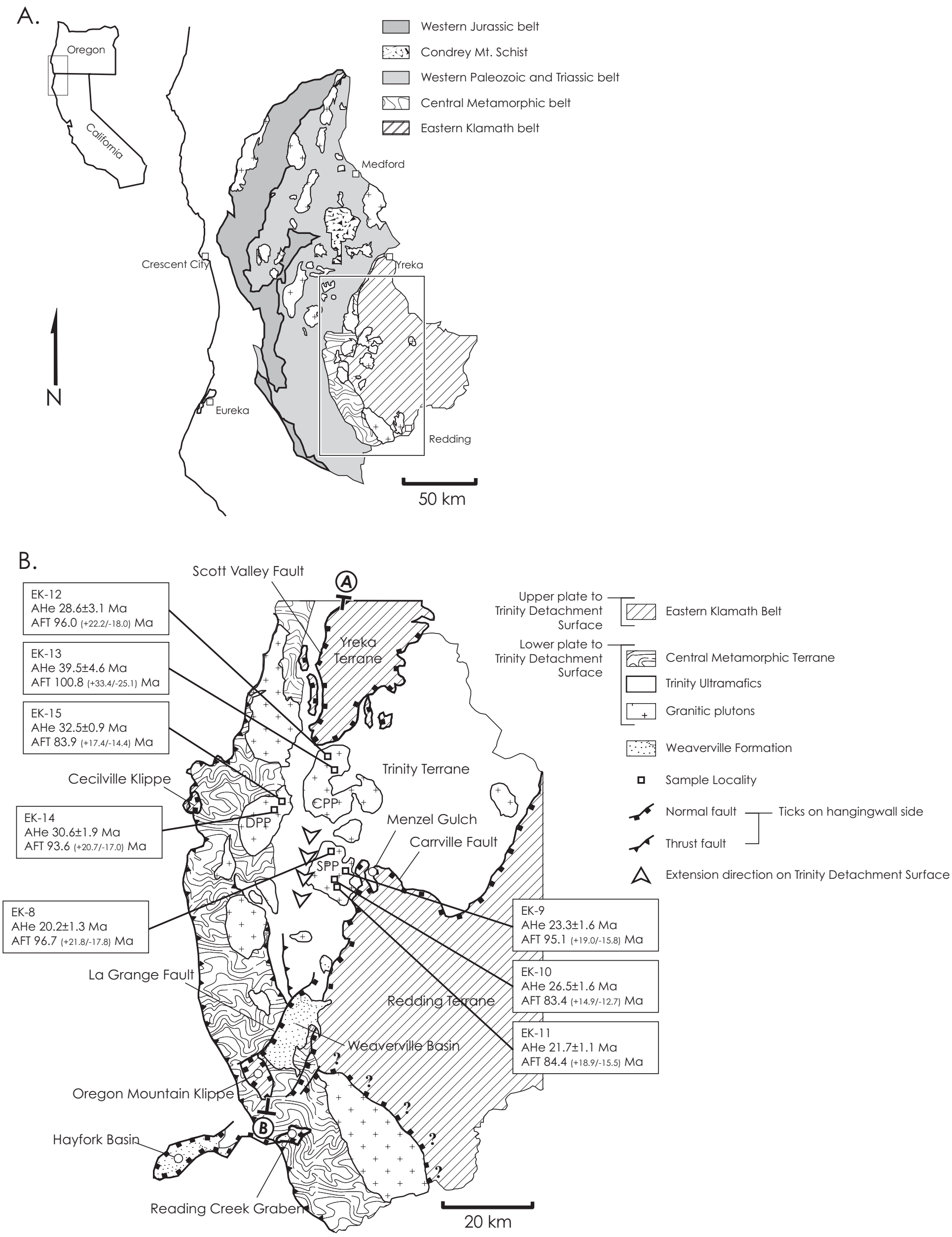

Fig. 1. (A) Simplified geological map of the Klamath region, modified from Irwin (1994). Inset box indicates Eastern Klamath region enlarged in panel B. (B) Sample localities dated in this study are shown as labelled squares. Line A-B illustrates the location and orientation of the cross section constructed in figure 6. DPP, CPP, and SPP mark the Deadmans Peak, Castle Peak, and Sugar Pine Peak Plutons, respectively.

The faults that collectively make up the Trinity Detachment Surface (fig. 1) juxtapose ttg suite plutons and their greenschist-amphibolite facies host rocks against a hanging wall assemblage that includes unmetamorphosed Paleozoic and poorly consolidated middle Tertiary sediments (Cashman and Elder, 2002; Fudge and Cashman,

TABLE 1

Sample locality and lithology information

Sample number	Latitude (°N)	Longitude (°W)	Elevation (m a.s.l.)	Intrusive body	Lithology	Crystallization age
EK-8	41° 3.42'	122° 45.33'	1372	Sugar Pine pluton	Granite	136.3±1.0 Ma[1]
EK-9	41° 2.80'	122° 47.83'	1938			
EK-10	41° 2.72'	122° 47.83'	2012			
EK-11	41° 6.80'	122° 48.25'	988			
EK-12	41° 16.00'	122 °49.50'	1231	Craggy Peak pluton	Granite	136.6±1.4 Ma[1,2]
EK-13	41° 14.00'	122° 47.00'	2048			
EK-14	41° 11.50'	122° 55.07'	1841	Deadman Peak pluton	Granite	142.3±1.1 Ma[1,2,3]
EK-15	41° 11.43'	122° 55.17'	2164			

SOURCES:
1. Allen and Barnes (2006).
2. Barnes and others (1996).
3. Wright and Fahan (1988).

2006; Fudge, ms, 2008). Prominent shallowly plunging slickenside striations on the fault surfaces argue for top-to-the-south extension towards a SSE to SSW direction, at a high angle to the accretionary fabric of the Klamath province (Cashman and Elder, 2002) (fig. 1). The mineralogy of syntectonic vein fill in cataclastic rocks capping the footwall of the La Grange Fault (fig. 1) is consistent with active slip at a maximum depth of c. 7km (Cashman and Elder, 2002).

Tertiary sedimentary rocks near the southern margin of the Klamath Mountains record motion on the La Grange fault, and also provide a limited record of Tertiary topographic relief through their changing sedimentary facies, detrital compositions, and pollen flora. Sandstone, conglomerate, shale, lignite and tuff of the Weaverville Formation are preserved in several small basins and grabens in the southern Klamath Mountains (MacGinitie, 1937; Irwin, 1963; Barnett, 1989; Phillips, ms, 1989; Phillips and Aalto, 1989) (fig. 1). In the Weaverville Basin itself, fluvial sediments are interbedded with debris flow deposits that thicken and coarsen toward the La Grange Fault, and contain clasts derived from Klamath bedrock units; together these characteristics indicate syn-depositional faulting (Phillips, ms, 1989; Phillips and Aalto, 1989). At the La Grange Mine, on the northwestern margin of the Weaverville Basin (fig. 1), gold-bearing gravels of the Weaverville Formation dip shallowly (~10°) towards, and are truncated by, the La Grange Fault (MacDonald, 1910; Schweickert and Irwin, 1989). Although no palynological data are available from the Weaverville Formation in the Weaverville Basin itself, pollen flora from Weaverville rocks in the Reading Creek and Hayfork basins are Early to early middle Miocene in age, and include a variety of species indicative of a landscape of moderate relief (Barnett, 1989). The Weaverville Formation unconformably overlies Lower Cretaceous marine mudstone and sandstone in the Reading Creek Basin, where both units have nearly parallel dips (Irwin, 1963; Cashman, unpublished data) suggesting that little to no post-Cretaceous tilting of the basin occurred prior to deposition of Weaverville Formation sediments.

FISSION-TRACK AGES

Apatite fission-track (AFT) ages were determined for eight samples collected from three tonalite-trondhjemite suite (ttg) plutons which collectively span the structural

TABLE 2

Results of apatite fission-track analyses

Sample	No. of grains	Fossil Track Density[1,2] ($x10^5/cm^2$)	Induced Track Density[1,2] ($x10^6//cm^2$)	U (ppm)	%Var	Chi square (%)	Age (Ma, $\pm 2\sigma$)	Mean Confined Fission Track Length (μm)	Standard deviation of the track length distribution (μm)	Number of tracks
EK-8	15	5.36 (306)	8.73 (499)	10.2	1.0	10	$96.7^{+21.8}_{-17.8}$ [3]	12.2	2.04	44
EK-9	15	10.8(506)	18.0 (845)	20.9	1.7	9	$95.1^{+19.0}_{-15.8}$ [3]	13.5	2.16	100
EK-10	30	10.1 (963)	19.3 (1847)	22.2	14.9	1	$83.4^{+14.9}_{-12.7}$ [3]	12.4	2.00	50
EK-11	15	5.65 (287)	10.8 (551)	12.3	1.1	6	$84.4^{+18.9}_{-15.5}$ [3]	N/A	N/A	-
EK-12	15	5.46 (266)	9.38 (457)	10.5	1.0	48	$96.0^{+22.2}_{-18.0}$ [3]	12.8	1.84	50
EK-13	6	5.08 (99)	8.37 (163)	9.3	1.5	99	$100.8^{+33.4}_{-25.1}$ [3]	13.8	1.48	26
EK-14	8	11.7 (303)	20.8 (541)	22.9	2.1	77	$93.6^{+20.7}_{-17.0}$ [3]	14.1	1.23	11
EK-15	14	8.36 (380)	16.8 (762)	18.4	1.4	28	$83.9^{+17.4}_{-14.4}$ [3]	14.3	1.79	11

Parentheses enclose number of tracks counted. Induced track densities were measured on mica external detectors (geometry factor = 0.5), and fossil track densities were measured on internal mineral surfaces exposed by polishing of mounted samples. Concordance of grain age distribution is assessed by the chi-square test (Galbraith, 1981), which determines the probability that the counted grains belong to a single age population (within Poissonian variation). If the chi-square value is less than 5%, it is likely that the grains counted represent a mixed-age population with real age differences between single grains.

NOTES:

1. Brackets show number of tracks counted.
2. Induced track densities measured on mica external detectors (g=0.5) and fossil track densities on internal apatite surfaces.
3. Ages calculated using the zeta method, with zeta factor of 138.99±10.2 (1 s.e.), based on three zeta determinations from both the Fish Canyon Tuff and Durango apatite.

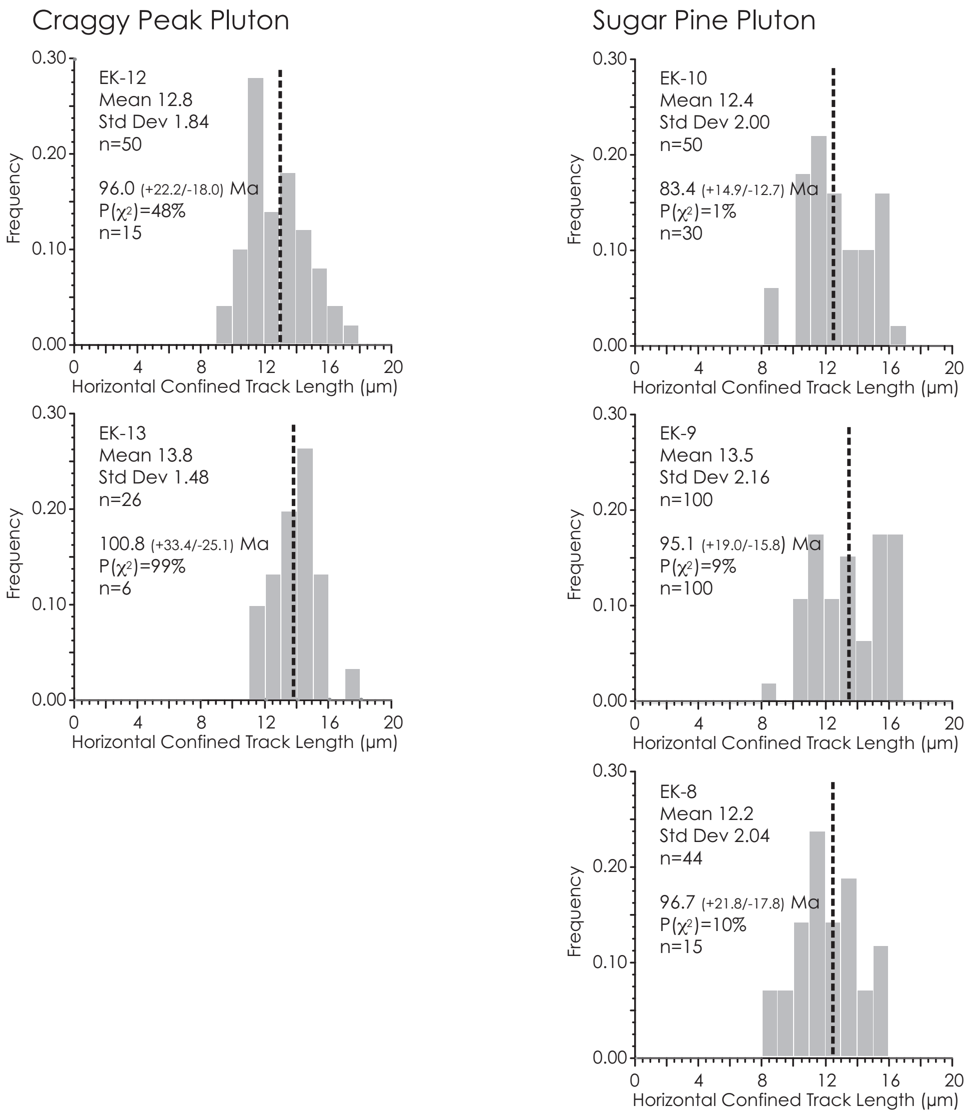

Fig. 2. Length distribution of horizontal confined fission tracks in apatite samples. Results are presented as relative frequency histograms with bin widths of 1μm.

window exposing lower plate rocks beneath the Trinity Detachment Surface—the "Trinity Arch" of Irwin and Lipman (1962) (fig. 1, table 1). Sampling sites were selected to include a range of elevations within each pluton, and to lie as close as possible to a single transect along the net extension direction measured on the faults making up the detachment surface (Cashman and Elder, 2002). Apatite grains from these samples typically exhibited a short aspect ratio (2 to 2.5:1 for unbroken grains) and were uniformly of excellent quality, with generally euhedral, optically transparent character.

Apatite fission-track analyses (table 2) were undertaken at Union College, following the protocols laid down in Brandon and others (1998), and described in Bigelow, ms, 1995. Details of the analytical methods used are described in the appendix.

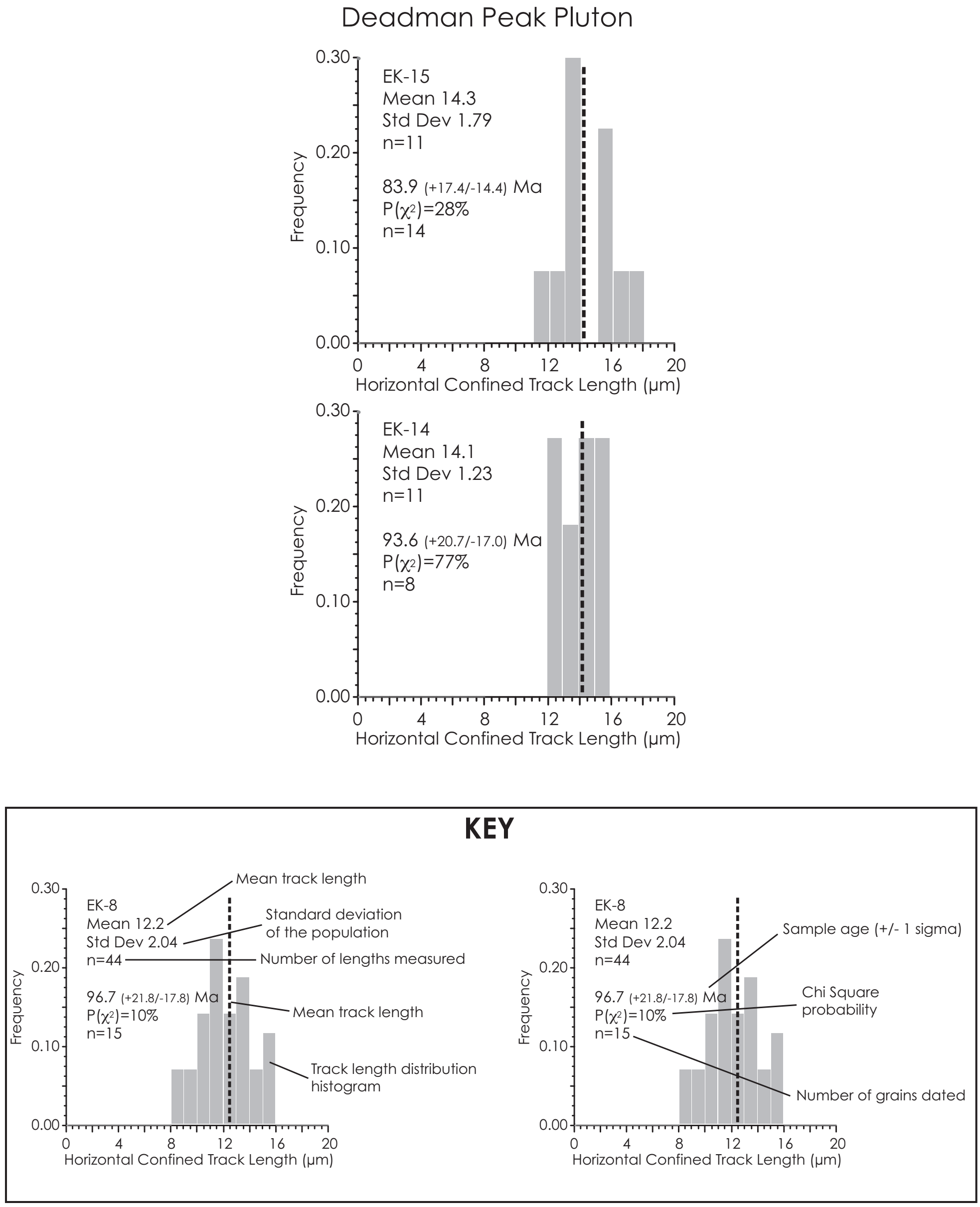

Fig. 2 (Continued).

Cretaceous ages were obtained for all samples, nominally varying between $83.4^{+14.9}_{-12.7}$ and $100.8^{+33.4}_{-25.1}$ Ma (2-sigma) although poor relative precision prevents any robust significance being attached to this range, with all ages lying within 2-sigma uncertainty of each other (table 2). Samples from the Sugar Pine (and to a lesser extent, Craggy Peak) Pluton exhibit substantial numbers of shortened tracks in the 8 to 12 μm length range. In the southern Sugar Pine Pluton in particular, the population of shortened tracks is significant enough to arguably define bimodal track length distributions for

TABLE 3

Apatite (U-Th)/He analyses

Pluton	Sample Number	Elevation (m)	Aliquot	^{4}He (ncc)	U (ppm)	Th (ppm)	Uncorrected age (Ma)	F_T	F_T Corrected Age (Ma)	Analytical uncertainty (Ma, 2σ)	Mass-weighted mean age (Ma)	Standard error (Ma, 2σ)
Sugar Pine Pluton	EK-8	1372	A	0.438	9.764	21.757	14.26	0.71	20.22	1.30	N/A	
	EK-9	1938	A	0.801	17.045	26.761	17.98	0.74	24.43	1.84	23.29	1.61
			B	0.639	11.938	16.825	15.82	0.71	22.15	1.46		
	EK-10	2012	A	0.511	13.876	24.678	19.92	0.75	26.53	1.56	N/A	
	EK-11	988	A	0.302	11.214	22.330	16.39	0.73	22.45	1.42	21.67	1.10
			B	0.293	11.751	24.713	15.48	0.74	20.89	1.84		
Craggy Peak Pluton	EK-12	1231	A	0.331	9.47	12.403	24.04	0.77	31.22	0.98	28.61	3.08
			B	0.443	12.957	14.637	18.18	0.72	25.21	1.22		
			C	0.526	9.904	12.782	20.85	0.71	29.41	1.08		
	EK-13	2048	A	1.102	16.267	17.702	31.20	0.73	42.74	2.12	39.52	4.55
			B	0.669	10.269	10.965	25.99	0.72	36.30	1.46		
Deadman Peak Pluton	EK-14	1841	A	1.077	17.293	37.895	21.19	0.73	29.19	1.12	30.56	1.94
			B	1.421	21.474	64.828	23.85	0.75	31.93	1.38		
	EK-15	2164	A	0.781	17.429	20.843	24.013	0.75	31.89	1.42	32.50	0.86
			B	0.750	14.910	17.659	24.46	0.74	33.10	1.64		

Correction for helium loss by alpha ejection is compensated for by the geometrical F_T correction procedure of Farley (2002). F_T factors were calculated for individual grains before being combined to produce an overall aliquot correction factor based on percentage mass contribution of each grain (assuming the approximation of a cylindrical geometry and an average density for apatite of 3.19 g/cm^3). Following the approach of Clark and others (2005) individual aliquots were combined to produce mean ages and uncertainties for each sample. Analyses featuring release of significant helium during re-heating were rejected, resulting in lack of experimental duplication for EK-8 and EK-10. For these samples, the average reproducibility of replicated analyses from the dataset (7.2%) is assigned as an estimated uncertainty. More information on the detail of the experimental conditions and raw data are available from the authors on request.

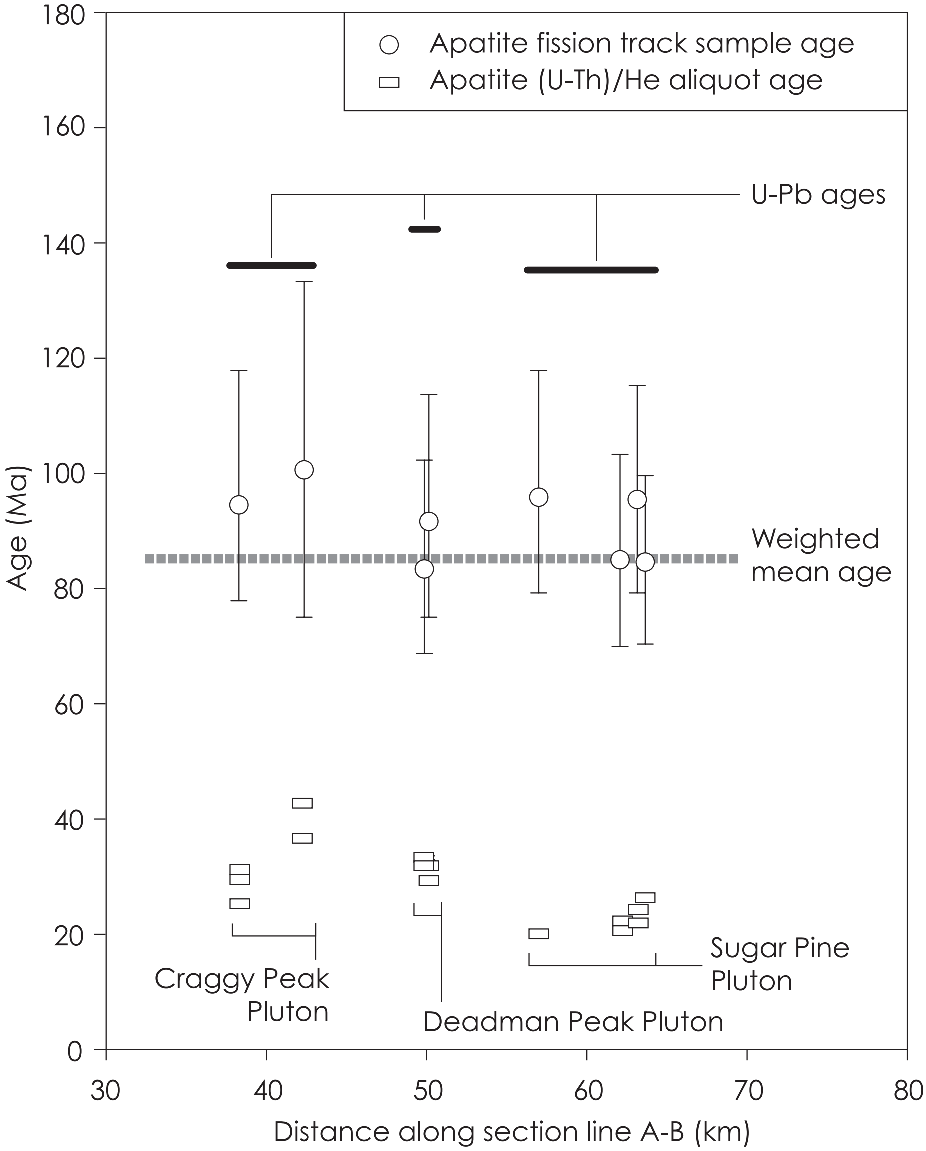

Fig. 3. Apatite fission track and (U-Th)/He age distribution plotted against distance along section line A-B (fig. 1), which is constructed along the trend of slickenside lineations preserved on remnants of the Trinity Detachment Surface.

samples EK-8, EK-9, and EK-10 (fig. 2). Although few short tracks are observed in EK-14 and EK-15 from the Deadman Peak pluton, the low number of measured tracks in these samples (table 2) leaves the implications of this statistically ambivalent.

APATITE (U-Th)/He AGES

All eight samples yielded sub-populations of euhedral, transparent apatite grains that were prepared for (U-Th)/He dating in the laboratory of Ken Farley at the California Institute of Technology.

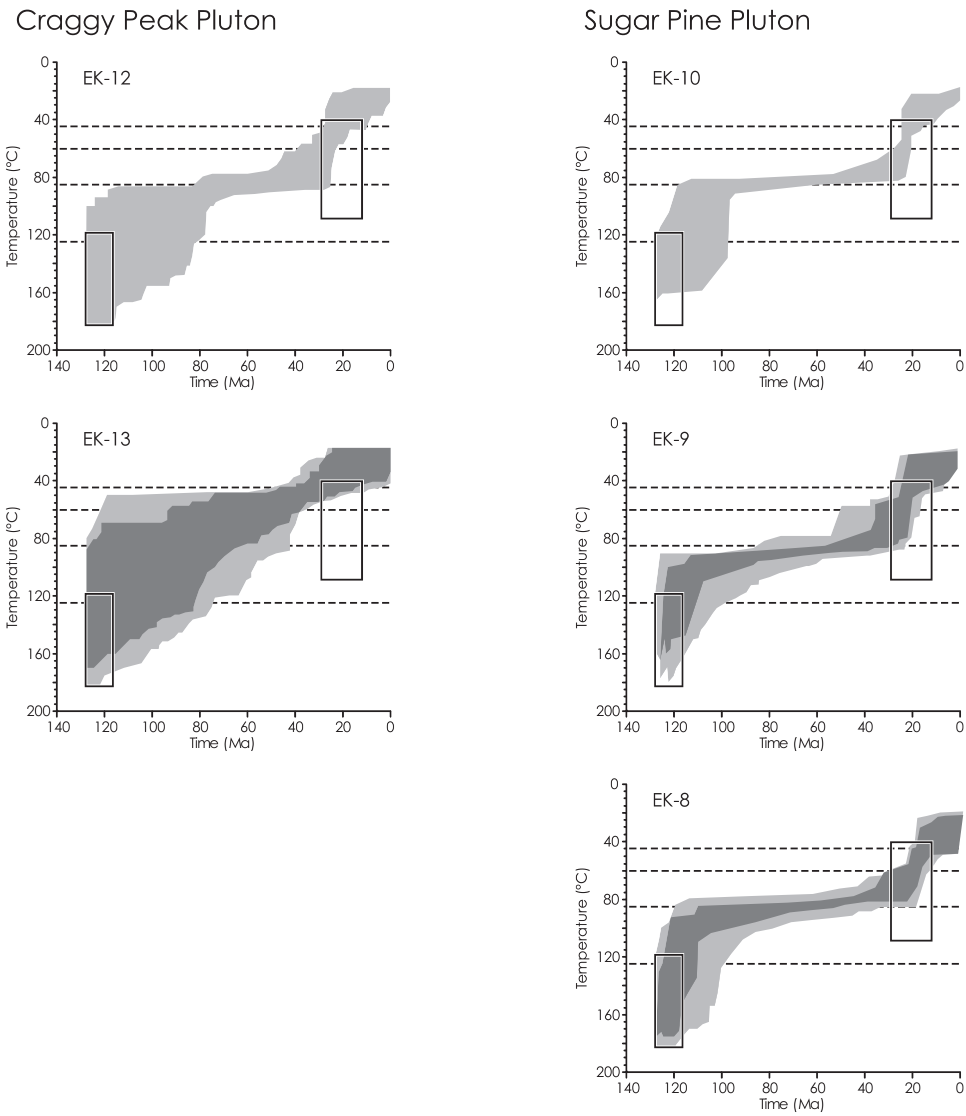

Fig. 4. Thermal histories derived from inverse modeling of combined track annealing and helium diffusion behavior in apatite using the HeFTy software package (Ketcham and others, 2000; Ketcham, 2005), constrained by apatite fission track age, horizontal confined track length distribution (uncorrected for angle to the C axis) and apatite (U-Th)/He age of samples. Annealing–diffusion algorithms used are those from Ketcham and others (1999). The light and dark gray envelopes represent the parametric bounds of models producing goodness of fit to the data in excess of 0.05 and 0.5, respectively [defined as "acceptable" and "good" fits by convention (Ketcham, 2005)]. Black boxes mark parametric limits placed on the models on the basis of regional stratigraphic and structural assumptions, as discussed in the text. Random sub-segment spacing was used, and no continuous cooling constraint was applied.

Selected euhedral apatite crystals were evaluated under an optical microscope, with any displaying fluid or crystalline inclusions rejected from analysis. Multi-grain aliquots comprising 6 to 10 hand-picked inclusion-free grains were encapsulated in steel casings. Helium was extracted by heating in a resistance furnace for 15 minutes at 900°C, and analyzed by isotope dilution on a Balzers QMG-064 quadrupole mass

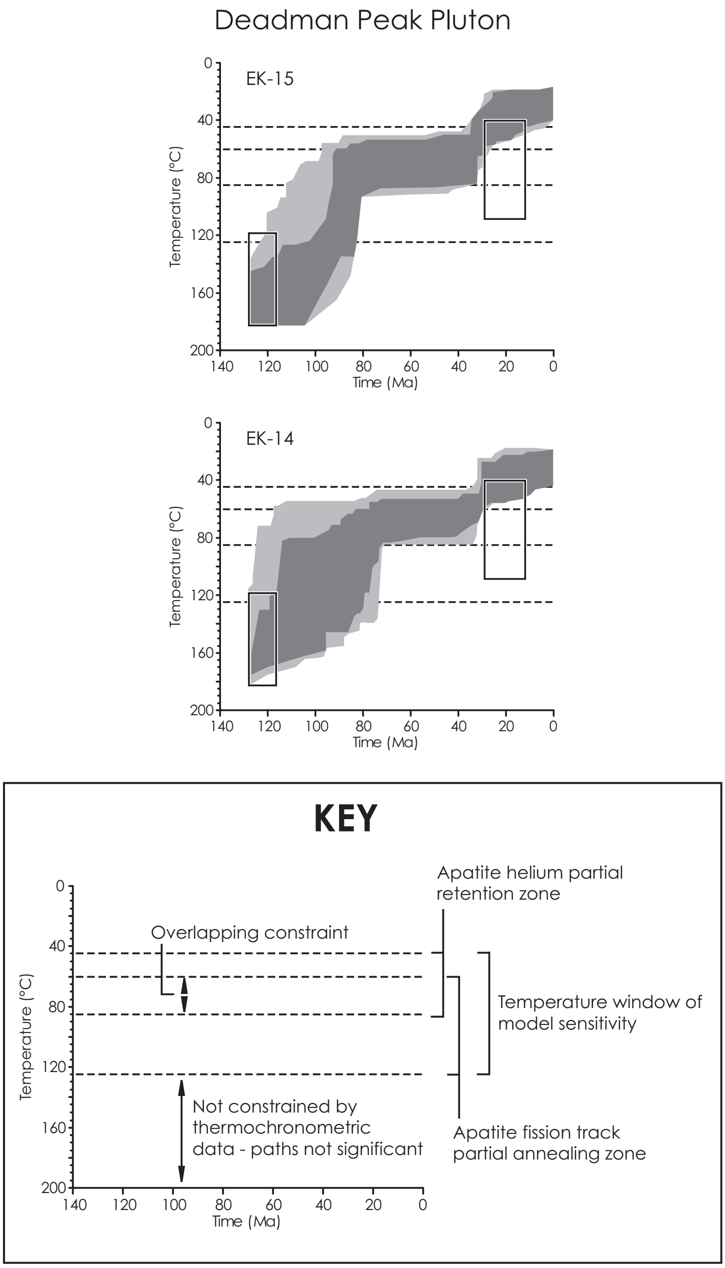

Fig. 4 (Continued).

spectrometer using the techniques described in House and others (1997). Completion of helium extraction was assessed by re-heating of out-gassed samples to 900°C. Samples from which significant helium was released during this re-heating—where the difference between the volume of helium evolved during re-heating and the hot furnace blank was greater than 1 percent of the helium released in the initial sample extraction—were rejected from further interpretations.

Successfully outgassed samples were removed from the furnace, extracted from their steel capsules, and dissolved before analysis of U and Th on a Finnegan Element double-focussing ICPMS.

Helium loss by alpha ejection was compensated for through the geometrical F_T correction procedure of Farley (2002). F_T correction factors were calculated for individual grains and combined to produce an overall aliquot correction factor weighted by the percentage mass contribution of each grain (assuming the approximation of a cylindrical geometry and an average density for apatite of 3.19 g/cm^3).

Where replicate analyses were obtained (table 3), these were combined to produce weighted mean sample values as the preferred measure of population age, following the approach of Clark and others (2005). For samples EK-8 and EK-10, rejection of aliquots due to significant helium release during re-heating resulted in completion of only one successful analysis, and a corresponding inability to assess reproducibility (table 3). Reported errors represent estimated precision to one standard deviation.

These analyses yield Tertiary apatite (U-Th)/He ages displaying significant geographical variation from 20.2±1.3 Ma in the southerly Sugar Pine Pluton to 39.5±4.6 Ma in the northern Craggy Peak Pluton (fig. 3). Internally consistent age-elevation variation is also apparent (fig. 3, table 3), with ages at lower elevation younger than those higher within a given pluton.

THERMOTECTONIC CONSTRAINT OF STRUCTURAL AND EROSIONAL HISTORY

Fission-track analysis provides a means for reconstructing the thermal histories of rock samples within defined windows of temperature where fission tracks experience significant annealing on geological timescales within the relevant mineral. Helium retention within crystals is also sensitive to temperature, such that (U-Th)/He ages provide an independent source of sub-surface temperature constraint. For apatite, these constraints overlap, with windows of thermal response between approximately 60 and 125°C for fission tracks (for example Green and others, 1989; Dumitru, 2000), and 45 to 85°C for helium (for example, Farley, 2000). Assuming a geothermal gradient of 25°C/km (explained below) and surface temperatures of 10°C, these overlapping constraints are equivalent to a combined depth window of 4.6 to 1.4 km beneath the Earth's surface.

The presence of heulandite in syn-deformational vein fill suggests the Trinity Detachment Surface was active at temperatures of 240±40°C (Cashman and Elder, 2002), arguing that slip on this structure began earlier than recorded by fission tracks in apatite, which only begin to accumulate at temperatures below 120°C (fig. 4). Although limited in extent, Lower Cretaceous [Hauterivian age (130-134 Ma)—Imlay, 1960] strata of the Great Valley Group underlying the Tertiary Weaverville Formation in some hangingwall basins (Schweickert and Irwin, 1989) show no onlapping relationship to the detachment surface, and may thereby represent an upper age limit to extension (fig. 5).

As noted above, all eight of our samples yielded statistically indistinguishable fission track ages, with a mean age (weighted for the number of tracks counted for each sample) of 84.4 Ma. As this pre-dates the reduction in geothermal gradient and attendant cooling of the crust associated with Laramide shallow-angle subduction (Dumitru and others, 1991), our first-order interpretation of these data is that the footwall of the Trinity Detachment Surface was exhumed towards the surface in Early to mid-Cretaceous time, cooling through ~100°C at c. 84 Ma.

Although nominally consistent with continuation of the deeper offset identified on the Trinity Detachment Surface above (fig. 5), an objection to direct association of the apparent exhumation with movement on this structure is raised by a post-tectonic muscovite-bearing rhyolite dike cutting the detachment at Menzel Gulch (fig. 1),

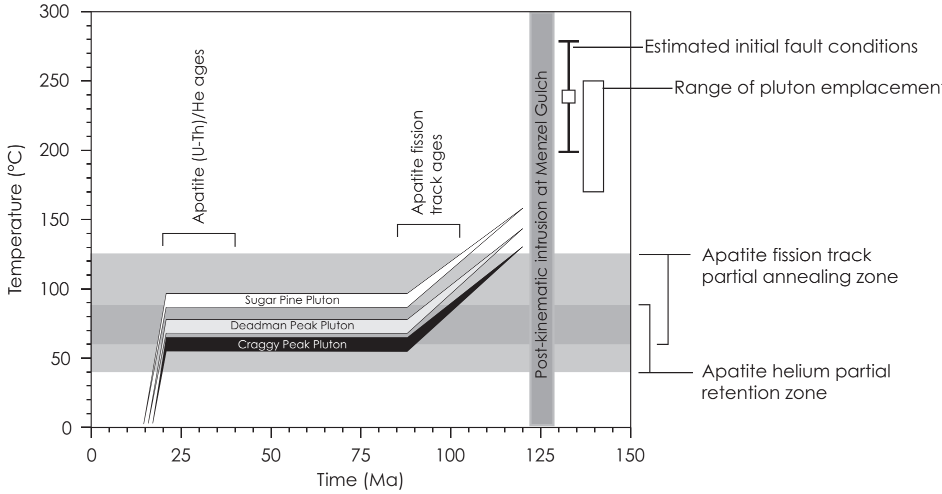

Fig. 5. Synthetic footwall thermal history summarizing available constraint of the sample array. Initial conditions are derived from syn-tectonic vein fill indicating La Grange Fault slip at temperatures of 240±40°C (Cashman and Elder, 2002). Reconciling the combined intra- and inter-sample thermochronological constraint requires two discrete episodes of cooling. Initial cooling in the Cretaceous must cease with the samples remaining within (or in the case of some Sugar Pine Pluton samples, possibly marginally below) the apatite helium partial retention zone.

which has yielded a K-Ar whole-rock age of 126±3 Ma (Cashman and Elder, 2002). Although this should be treated with caution in light of the ambiguities inherent in whole-rock K-Ar dating (McDougall and Harrison, 1999), taken at face value this age would require that active slip on the Trinity Detachment Surface to the south (and thereby down-dip) of the presently exposed footwall window ceased prior to our sample array cooling through temperatures allowing fission track retention (figs. 5 and 6).

This kinematic limit can be reconciled with the Cretaceous exhumation required by our new data in three ways. (1) Assuming the Trinity Detachment Surface operated as suggested by Cashman and Elder (2002)—with progressive initiation of new fault splays soling into the detachment surface as rotation led to the locking up of shallow fault structures—extension may have ceased on the Menzel Gulch strand prior to 126 Ma, but continued on fault strands farther south (fig. 6). (2) Active offset on the Trinity Detachment Surface may have ceased prior to 126 Ma, but with post-faulting exhumation continuing due to erosional lowering of the uplifted footwall block, or (3) The K-Ar age may be in error due to the presence of excess argon or other problematic sample behavior not resolvable under this analytical approach.

The Cretaceous sedimentary record of the Klamath region is too fragmentary to test the relative implications of these scenarios (Nilsen, 1984), but whichever is accepted, the populations of shortened tracks (fig. 2) and significantly younger (U-Th)/He ages obtained suggest that our samples either remained buried within the fission track partial annealing zone at the end of this Cretaceous episode of exhumation, at temperatures high enough to allow the apatite crystal structure to remain partially to completely open to the diffusive loss of helium (figs. 4 and 5), or were subsequently re-heated to such temperatures. In the absence of evidence for burial of the footwall region examined here, we prefer the first of these alternatives as the more parsimonious explanation of the data.

Lack of direct constraint on the structural elevation of the now eroded Trinity Detachment Surface above our sampled localities leaves open the question of whether

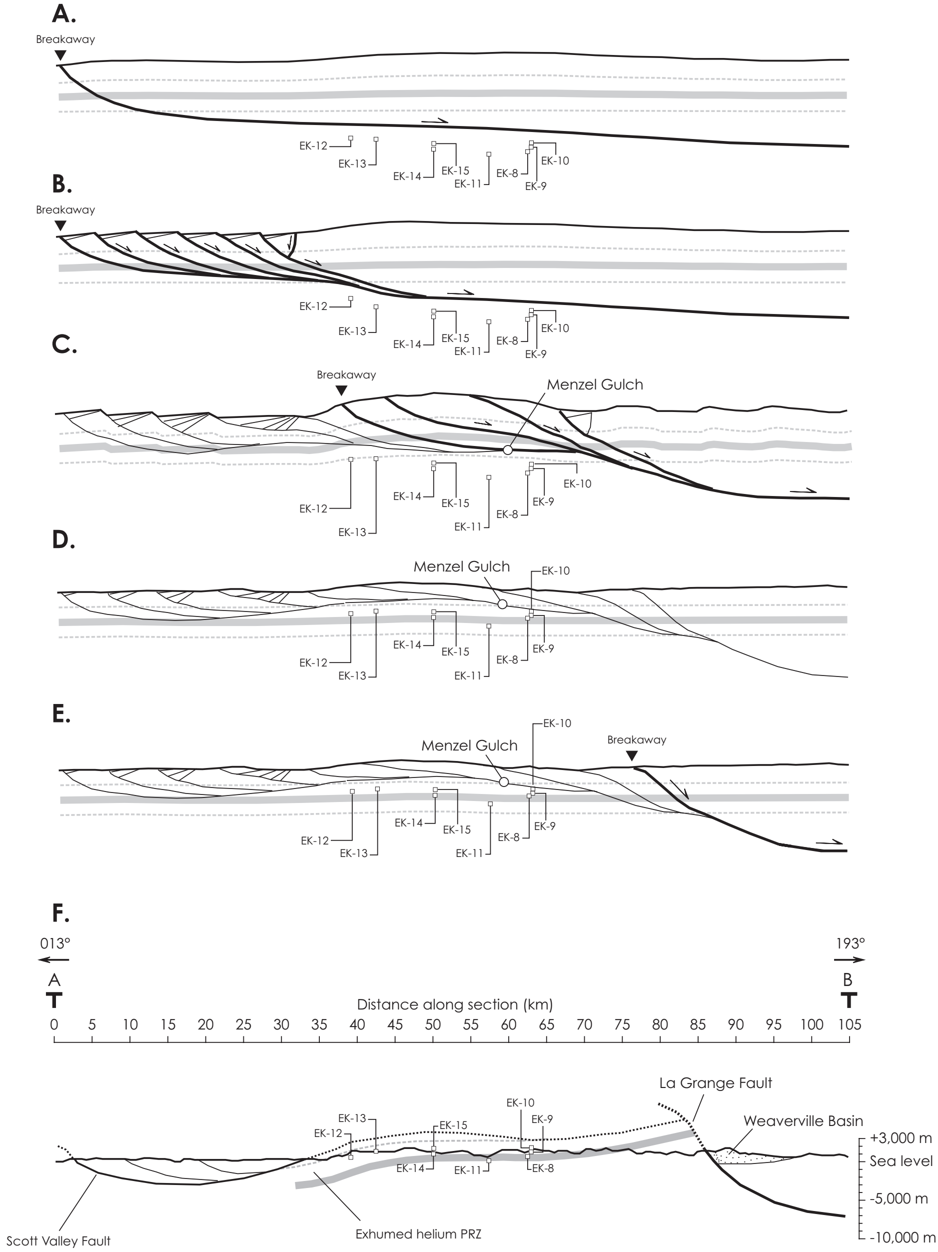

Fig. 6. Structural evolution synthesized from thermochronometric constraint and geological evidence. Kinematic style for the sequence A-E is based on the model of Cashman and Elder (2002), after Spencer (1984). Relative sample location is illustrated with respect to the key contemporary thermochronological behavioral domains shown in gray, with the base of the partial annealing zone for fission tracks and the upper limit of the partial retention zone for helium in apatite indicated by the lower and upper dashed lines, respectively, and the transitional zone between these behavioral domains shown by the thicker solid line. (A) Inception of detachment fault—early Cretaceous. (B) As extension progresses, upper crustal deformation leads to development of further sympathetic faults, and rotation of upper-plate faults leads to synformal upwarping of the lower plate. (C) Post-kinematic intrusion on the fault surface at Menzel Gulch may constrain the local end of the Cretaceous slip episode as prior to 126±3 Ma, but (D) continued exhumation after this point is required to reconcile our fission track data. Fission track length distributions and helium data require that our footwall samples remain 2–3 km deep within (and notably for the Sugar Pine Pluton,

the lower plate may have been completely unroofed during this Cretaceous episode, but the close proximity of the Scott Valley Fault—which likely represents a northern remnant of the Trinity Detachment Surface (Cashman and Elder, 2002)—to the Craggy Peak Pluton (fig. 1) favors the presence of a carapace of upper plate Eastern Klamath Belt rocks at the end of the Cretaceous, at least in the north of the sampled area (fig. 6).

To develop a more precise interpretation, combined constraint from seven of our samples yielding adequate fission track data was simulated using the HeFTy modeling code (Ketcham and others, 2000; Ketcham, 2005) (fig. 4). This program tests observed fission track and helium age data for apatite against empirical temperature responses calibrated against laboratory and borehole heating experiments, allowing the relative merit of different thermal histories to be assessed. For our samples, three limits were imposed on Cenozoic history, based on regional stratigraphic data: (1) the sampled footwall areas were exhumed by faulting on the Trinity Detachment Surface commencing at c. 130 Ma; (2) late Cenozoic exhumation and cooling of samples commenced in the early Miocene, coincident with the reactivation of the La Grange fault; and (3) the samples are at the Earth's surface today.

The families of thermal histories producing statistically acceptable fits to the combined thermochronometric datasets of these seven samples (fig. 4) exhibit three common elements: (1) relatively rapid cooling into the apatite fission track partial annealing zone during the Early to mid Cretaceous; (2) a period of relative thermal stability at or around the range of overlapping temperature sensitivity between the two chronometers; and then (3) renewed cooling through the window of variable helium retention in the later Tertiary (fig. 4). Conservation of these basic elements across the full array of samples reinforces our confidence that they reflect real and significant aspects of regional history.

The principle factor varying between the modeled thermal histories is the relative temperature at which different samples stabilized between the Cretaceous and Tertiary cooling episodes, which nominally increases from north to south (consistent with the structural arguments of Cashman and Elder, 2002). In particular, due to their extended residence at temperatures allowing the annealing of fission tracks and/or the diffusive loss of helium, samples from the northern Craggy Peak and Deadmans Peak plutons exhibit poor precision on the timing of both cooling episodes, although remaining consistent with the tripartite thermal history defined for the southern Sugar Pine Pluton samples (fig. 4).

The diachronous accumulation of strata in the Reading Creek graben (fig. 1) supports this modeled history, arguing against the majority of the apatite (U-Th)/He ages encountered here directly reflecting post-Cretaceous exhumation and cooling. Significant regional unroofing between the end of the Cretaceous episode and the Early to Middle Miocene age of the Weaverville Formation would likely have disturbed and rotated strata of the Cretaceous Great Valley Group, thereby resulting in an angular discordance between Cretaceous and Miocene strata, rather than the paraconformable relationship observed (Cashman and Elder, 2002).

Such an interpretation is consistent with the main array of helium ages representing an exhumed Cretaceous-Miocene helium partial retention zone (PRZ), as sug-

possibly marginally below) the apatite helium partial retention zone at the cessation of this exhumation episode. (E) Initiation of Miocene exhumation. The La Grange Fault segment is active to the south, but the Menzel Gulch intrusion nominally rules out reactivation above the sampled lower plate region, implying that the exhumation indicated for our samples is largely erosional in its immediate cause. (F) Eastern Klamath Mountains today, after Cashman and Elder (2002). Structural cross-section constructed along line A-B shown in figure 1.

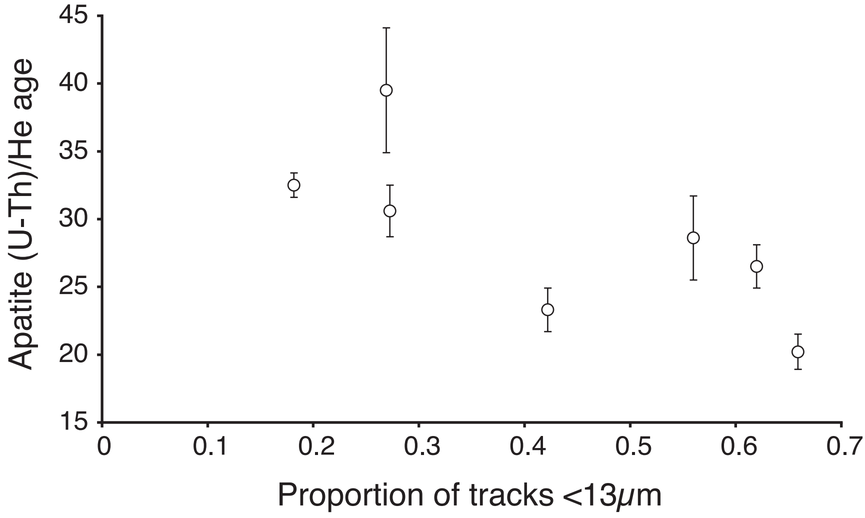

Fig. 7. Relative abundance of shortened fission tracks plotted against helium age for our sample array. For the purposes of this distinction, shortened tracks are defined as those with a measured length of less than 13 μm. When held at temperatures within the range of thermal sensitivity overlap between helium retention and fission track annealing (fig. 4) for a significant period, fission track length and helium age in apatite should both be observed to decrease with structural depth (Stockli and others, 2000).

gested by our modeling of the thermochronological response of these samples (fig. 4). The PRZ corresponds to a limited depth interval in the upper crust across which ambient temperature varies between hot enough for all the atoms of a given radiogenic isotope produced in a crystal to escape via diffusional processes, and cold enough for diffusional transport to effectively cease for the relevant lattice structure (a range between ~85°C and 40°C, respectively, for helium in apatite), and thereby represents a potentially significant control on the magnitude of exhumation experienced. Samples held within such a zone for a period will build up a quasi-steady state gradient in age with depth, between zero at the deeper, higher temperature boundary (where no helium is retained on geological timescales) and some finite age reflecting 100 percent helium retention at the cooler end (Braun and others, 2006). Crucially, if these rocks are subsequently brought to the surface, samples exposed from structurally below the PRZ will record cooling ages related to the exhumation, but all material exposed from within the PRZ will yield ages pre-dating the exhumation episode.

Inverse correlation observed between the proportion of shortened apatite fission track lengths in our samples and their apatite (U-Th)/He ages (fig. 7) is also consistent with this interpretation. As demonstrated by Stockli and others (2000) in their seminal White Mountains study, apatite fission-track ages and mean track lengths begin to decrease towards the base of the helium partial retention zone. Although the lack of an independent structural datum prevents the direct identification of a comparable trend of varying fission track and helium retention with paleodepth for our data, the behavior identified by Stockli and others (2000) provides a template by which the spatial trends observed in our data (figs. 2 and 7) can be shown to be consistent with the southward-deepening structural exhumation predicted by the structural model of Cashman and Elder (2002).

Speculatively, the interpretation that at least some parts of the Sugar Pine pluton may have been exhumed from below the helium partial retention zone for apatite in the later Tertiary (fig. 4) imbues these samples with added significance. Moving from below the deeper to above the shallower limit of the helium PRZ (approximately 85 and 40°C, respectively, as noted above) would require at least 45°C of cooling. Assuming a pre-Miocene geothermal gradient of 25°C/km, this corresponds to at least 1.8 km of exhumation during this episode.

Exhumation from below the helium PRZ (where ages remain perpetually held at zero by the rapid diffusive loss of helium) would also require that the ages of affected samples relate directly to the Tertiary cooling episode—unlike those with extended residence within the PRZ. Clustering of the structurally lower three of our Sugar Pine Pluton sample in the range 20 to 23 Ma thereby suggests an Early Miocene initiation for this phase of exhumation.

Although we remain cautious on such higher-order points of interpretation, this would be internally consistent with the apparent trends in relative exhumation depth and corresponding helium and fission track retention across our sample array (figs. 4 and 6), with Sugar Pine Pluton as the southernmost, and by inference from the structural model of Cashman and Elder (2002) the most deeply exhumed of the three footwall plutons sampled.

Within the limits provided by the syn-deformational sediments of the Weaverville Basin (fig. 1), this thermochronological record of exhumation correlates to the Tertiary offset on the La Grange Fault, which forms the southern boundary to the exposed Trinity Arch (fig. 1). Although such juxtaposition may suggest a kinematic relationship between Tertiary exhumation of our samples and slip on the La Grange Fault, the residence of these samples within the brittle upper crust during the early Tertiary (as discussed above) argues against renewed mid-Tertiary slip on the detachment surface above the Trinity Arch, which by this time is assumed to have been rotated to a low-angle highly unsuited to active slip (fig. 6). As noted above, the nominally mid-Cretaceous post-tectonic intrusion cutting the Trinity Detachment Surface at Menzel Gulch also argues against Tertiary reactivation of the wider structure.

Instead, we must assume that renewed faulting occurred on only that portion of the La Grange fault bounding the Weaverville basin, with the contemporaneous exhumation and exposure of our samples representing erosional modification of the uplifted footwall proximal to this structure (fig. 6).

CONCLUSIONS

Our new apatite fission-track and, particularly, (U-Th)/He data provide a window into the latest Mesozoic and Cenozoic evolution of the eastern Klamath Mountains, allowing us to deconvolve multiple tectonic episodes superimposed on the region during this period of rapidly evolving plate boundary conditions at the western margin of North America. At least two episodes of extension and syn/post-slip erosion of all or part of the Trinity Detachment Surface are required to fully account for the observed distribution of ages across our sample array, one in the mid-Cretaceous and one in Early Miocene time.

Although Cretaceous slip on at least some segments of the low-angle Trinity Detachment Surface may have ceased by 126±3 Ma, exhumation—attributable to southward propagation of active fault splays and/or post-tectonic erosional lowering of the landscape—continued until approximately 80 Ma, and was ultimately responsible for exhumation of rocks currently exposed in the footwall of the structure to temperatures of between 65 and 80°C.

The possible exposure of an exhumed apatite helium partial retention zone argues strongly for Late Cretaceous to (at least) Late Paleogene quiescence and stability of this region. This PRZ was disrupted and unroofed by at least 1.8 km of subsequent Miocene exhumation, tentatively dated as initiating at c. 20 to 23 Ma.

Shallow crustal residence of the footwall rocks rules out widespread reactivation of the integrated detachment structure, and suggests that this second episode of exhumation experienced by our samples must be primarily attributed to erosion. However, this activity is contemporaneous with renewed extension along the La Grange Fault immediately to the south.

We note that this putative early Miocene age would associate reactivation of the La Grange Fault with a range of widespread volcanic and structural changes across the western Cordillera region preceding development of Basin and Range extension (for example, Gans and others, 1985; Colgan and others, 2006). Although such a link is speculative, this would represent the first time such activity has been recognized in the Coastal Range systems of western North America.

Retention of Cretaceous apatite fission-track and Oligocene-Miocene (U-Th)/He ages in the exposed footwall plutons require that the present high topography and relief of the Klamaths represents a juvenile landscape that has not yet produced a resolvable thermochronological signal in the exposed surface geology. The effects of this rejuvenation have thus far been limited to surface uplift and attendant relative base level lowering, resulting in the incision of substantial local relief into the formerly subdued topography. The notable preservation of Pliocene and Tertiary landscape elements in the uplifted sequence (Diller, 1902; Stone and others, 1993; Aalto and others, 1998; Aalto, 2006) argues for little overall surface lowering during this episode.

ACKNOWLEDGMENTS

This research was made possible by support from NERC grant NER/M/S/2002/00097, and by a grant to Batt from the American Chemical Society Petroleum Research Fund. Irradiation was facilitated by the US DOE RUS grant awarded to Oregon State University. This manuscript benefitted from reviews by Trevor Dumitru and Rebecca Flowers.

Appendix—analytical methods

Apatite fission-track analyses (table 1) were undertaken at Union College, following the protocols laid down in Garver and Brandon (1994). Apatite was isolated from c. 5 kg disaggregated samples by initial density concentration on a Rogers Table, followed by standard heavy liquid (tetrabromoethane and methylene iodide) and magnetic separation techniques. 10 to 20 mg aliquots of apatite were mounted in epoxy on glass slides and polished to expose internal grain surfaces. Spontaneous fission tracks were revealed by etching for 20 seconds in 5M HNO_3 at $\sim$20°C. Prepared mounts were covered by a thin sheet of low uranium muscovite secured by tape to serve as a detector for neutron-induced ^{235}U fission fragments. Samples were irradiated with thermal neutrons at the Oregon State University TRIGA reactor in Corvallis, with two pieces of the Corning Glass standard CN1 included at the ends of the irradiation package. Neutron fluence experienced by the samples was on the order of 8×10^{15} cm^{-2}. Mica detectors were etched in 40 percent HF for 15 min. Ages were calculated using a weighted mean zeta calibration factor (Fleischer and others, 1975; Hurford and Green, 1983) for standard apatites from the Fish Canyon Tuff, Durango, and the Mount Dromedary quartz monzonite (Miller and others, 1985). Track densities of both spontaneous and induced tracks were measured on an Olympus BH-2 microscope at $\times$1562 magnification ($\times$100 dry objective, $\times$1.25 microscope tube, $\times$12.5 oculars) objective. Length measurements were carried out on the same optical system in conjunction with a Calcomp digitizing tablet interfaced with a Mac IIci computer.

(U-Th)/He dating of apatite samples was undertaken in the laboratory of Ken Farley at the California Institute of Technology. Selected euhedral apatite crystals were evaluated under an optical microscope, with any displaying fluid or crystalline inclusions visible at $\times$90 magnification rejected from analysis. Multi-grain aliquots comprising 6 to 10 hand-picked inclusion-free grains were encapsulated in steel casings. Helium was extracted by heating in a resistance furnace for 15 minutes at 900°C, and analyzed by isotope dilution on a Balzers QMG-064 quadrupole mass spectrometer using the techniques described in House and others (1997). Outgassed samples were removed from the furnace, extracted from their steel capsules for evaluation, and dissolved before analysis of U and Th on a Finnegan Element double-focussing ICPMS.

Helium loss by alpha ejection was compensated for through the geometrical F_T correction procedure of Farley (2002). F_T correction factors were calculated for individual grains and combined to produce an overall aliquot correction factor weighted by the percentage mass contribution of each grain (assuming the approximation of a cylindrical geometry and an average density for apatite of 3.19 g/cm^3).

Further details of each of these experimental methods are available from the authors on request.

References

Aalto, K. R., 2006, The Klamath peneplain; A review of J. S. Diller's classic erosion surface, *in* Snoke, A. W., and Barnes, C. G., editors, Geological studies in the Klamath Mountains Province, California and Oregon: A Volume in Honor of William P. Irwin: Geological Society of America Special Paper 410, p. 451–463, doi:10.1130/2006.2410(22).

Aalto, K. R., Sharp, W. D., and Renne, P. R., 1998, ^{40}Ar/^{39}Ar dating of detrital micas from Oligocene-Pleistocene sandstones of the Olympic Peninsula, Klamath Mountains, and northern California Coast Ranges: Provenance and paleodrainage patterns: Canadian Journal of Earth Sciences, v. 35, p. 735–745, doi:10.1139/cjes-35-7-735.

Allen, C. M., and Barnes, C. G., 2006, Ages and some cryptic sources of Mesozoic plutonic rocks in the Klamath Mountains, California and Oregon, *in* Snoke, A. W., and Barnes, C. G., editors, Geological studies in the Klamath Mountains Province, California and Oregon: A volume in honor of William P. Irwin: Geological Society of America Special Paper 410, p. 223–245, doi:10.1130/2006.2410(11).

Barnes, C. G., Petersen, S. W., Kistler, R. W., Murray, R., and Kays, M. A., 1996, Source and tectonic implications of tonalite-trondhjemite magmatism in the Klamath Mountains: Contributions to Mineralogy and Petrology, v. 123, p. 40–60, doi:10.1007/s004100050142.

Barnett, J., 1989, Palynology and paleoecology of the Tertiary Weaverville Formation, northwestern California, U.S.A.: Palynology, v. 13, p. 195–246.

Bigelow, J. J., ms, 1995, Fission-track ages of plutons in the footwall of the LaGrange fault, Klamath Mountains: Schenectady, New York, Union College, unpublished senior thesis, 44 p.

Brandon, M. T., Roden-Tice, M. K., and Garver, J. I., 1998, Late Cenozoic exhumation of the Cascadia accretionary wedge in the Olympic Mountains, northwest Washington State: Geological Society of America Bulletin, v. 110, p. 985–1009, doi: 10.1130/0016-7606(1998)110<0985:LCEOTC>2.3.CO;2.

Braun, J., van der Beek, P., and Batt, G. E., 2006, Quantitative Thermochronology: Cambridge, Cambridge University Press, 272 p.

Brudzinski, M. R., and Allen, R. M., 2007, Segmentation in episodic tremor and slip all along Cascadia: Geology, v. 35, p. 907–910, doi:10.1130/G23740A.1.

Cashman, S. M., 1988, Finite-strain patterns of Nevadan deformation, western Klamath Mountains, California: Geology, v. 16, p. 839–843, doi:10.1130/0091-7613(1988)016<0839:FSPOND>2.3.CO;2.

Cashman, S. M., and Elder, D. R., 2002, Post-Nevadan detachment faulting in the Klamath Mountains, California: Geological Society of America Bulletin, v. 114, p. 1520–1534, doi:10.1130/0016-7606(2002)114<1520:PNDFIT>2.0.CO;2.

Clark, M. K., House, M. A., Royden, L. H., Whipple, K. X., Burchfiel, B. C., Zhang, X., and Tang, W., 2005, Late Cenozoic uplift of southeastern Tibet: Geology, v. 33, p. 525–528, doi: 10.1130/G21265.1.

Colgan, J. P., Dumitru, T. A., Reiners, P. W., Wooden, J. L., and Miller, E. L., 2006, Cenozoic tectonic evolution of the Basin and Range Province in northwestern Nevada: American Journal of Science, v. 306, p. 616–654, doi:10.2475/08.2006.02.

Davis, G. A., Holdaway, M. J., Lipman, P. W., and Romey, W. D., 1965, Structure, metamorphism and plutonism in the south-central Klamath Mountains, California: Geological Society of America Bulletin, v. 76, p. 933–966, doi:10.1130/0016-7606(1965)76[933:SMAPIT]2.0.CO;2.

Davis, G. A., Ando, C. J., Cashman, P. H., and Goullaud, L., 1979, Cross-section of the central Klamath Mountains: Geological Society of America Map and Chart Series MC-28I.

Diller, J. S., 1902, Topographic development of the Klamath Mountains: U.S. Geological Survey, Bulletin, v. 196, 69 p.

Dumitru, T. A., 2000, Fission-track geochronology, *in* Noller, J. S., Sowers, J. M., and Lettis, W. R., editors, Quaternary geochronology; methods and applications: American Geophysical Union Reference Shelf, v. 4, p. 131–155.

Dumitru, T. A., Gans, P. B., Foster, D. A., and Miller, E. L., 1991, Refrigeration of the western Cordilleran lithosphere during Laramide shallow-angle subduction: Geology, v. 19, p. 1145–1148, doi:10.1130/0091-7613(1991)019<1145:ROTWCL>2.3.CO;2.

Ernst, W. G., Snow, C. A., and Scherer, H. H., 2008, Contrasting early and late Mesozoic petrotectonic evolution of northern California: Geological Society of America Bulletin, v. 120, p. 179–194. doi: 10.1130/B26173.1

Evernden, J. F., and Kistler, R. W., 1970, Chronology of emplacement of Mesozoic batholithic complexes in California and western Nevada: U.S. Geological Survey Professional Paper 623, 42 p.

Farley, K. A., 2000, Helium diffusion from apatite: General behavior as illustrated by Durango fluorapatite: Journal of Geophysical Research-Solid Earth, v. 105(B2), p. 2903–2914, doi:10.1029/1999JB900348.

——— 2002, (U-Th)/He Dating: Techniques, Calibrations, and Applications: Reviews in Mineralogy and Geochemistry, v. 47, p. 819–844, doi:10.2138/rmg.2002.47.18.

Fleischer, R. L., Price, P. B., and Walker, R. M., 1975, Nuclear Tracks in Solids: Principles and Applications: Berkeley, California, University of California Press, 605 p.

Fudge, E. C., ms, 2008, Evidence for regional extensional faulting at Grey Rocks Ridge, Eastern Klamath Mountains, California: Arcata, California, Humboldt State University, M.S. Thesis, 97 p.

Fudge, E. C., and Cashman, S. M., 2006, Evidence for regional extensional faulting at Grey Rocks Ridge, eastern Klamath belt, Eastern Klamath Mountains, Shasta County, California: Geological Society of America Abstracts with Programs, v. 38, p. 18–19.

Galbraith, R. F., 1981, On statistical models for fission track counts: Mathematical Geology, v. 13, p. 471–478, doi:10.1007/BF01034498.

Gans, P. B., Miller, E. L., McCarthy, J., and Ouldcott, M. L., 1985, Tertiary extensional faulting and evolving ductile-brittle transition zones in the northern Snake Range and vicinity: New insights from seismic data: Geology, v. 13, p. 189–193, doi: 10.1130/0091-7613(1985)13<189:TEFAED>2.0.CO;2.

Garver, J. I., and Brandon, M. T., 1994, Erosional denudation of the British Columbia Coast Ranges as determined from fission-track ages of detrital zircon from the Tofino Basin, Olympic Peninsula, Washington: Geological Society of America Bulletin, v. 106, p. 1398–1412, doi:10.1130/0016-7606(1994)106<1398:EDOTBC>2.3.CO;2.

Goodge, J. W., 1989, Evolving early Mesozoic convergent margin deformation, central Klamath Mountains, Northern California: Tectonics, v. 8, p. 845–864, doi:10.1029/TC008i004p00845.

Green, P. F., Duddy, I. R., Laslett, G. M., Hegarty, K. A., Gleadow, A. J. W., and Lovering, J. F., 1989, Thermal annealing of fission tracks in apatite 4. Quantitative modelling techniques and extension to geological timescales: Chemical Geology, v. 79, p. 155–182.

Harper, G. D., Saleeby, J. B., and Heizler, M., 1994, Formation and emplacement of the Josephine ophiolite and the Nevadan orogeny in the Klamath Mountains, California-Oregon: U/Pb, ^{40}Ar/^{39}Ar geochronology: Journal of Geophysical Research-Solid Earth, v. 99(B3), p. 4293–4321, doi:10.1029/93JB02061.

House, M. A., Wernicke, B. P., Farley, K. A., and Dumitru, T. A., 1997, Cenozoic thermal evolution of the central Sierra Nevada, California, from (U-Th)/He thermochronometry: Earth and Planetary Science Letters, v. 151, p. 167–179, doi:10.1016/S0012-821X(97)81846-8.

Hurford, A. J., and Green, P. F., 1983, The zeta age calibration of fission-track dating: Chemical Geology (Isotope Geoscience Section), v. 1, p. 285–317, doi:10.1016/S0009-2541(83)80026-6.

Imlay, R. W., 1960, Ammonites of Early Cretaceous (Valanginian and Hauterivian) from the Pacific Coast States: U.S. Geological Survey Professional Paper P 0334-F, p. 167–228.

Irwin, W. P., 1963, Preliminary geologic map of the Weaverville Quadrangle, California: United States Geological Survey, Mineral Investigations Field Studies Map MF-0275, scale 1:62,500, 1 sheet.

——— 1972, Terranes of the western Paleozoic and Triassic belt in the southern Klamath Mountains, California, *in* Geological Survey Research 1972: U.S. Geological Survey Professional Paper 800-C, p. C103–C111.

——— 1985, Age and tectonics of plutonic belts in accreted terranes of the Klamath Mountains, California and Oregon, *in* Howell, D. G., editor, Tectonostratigraphic terranes of the circum-Pacific region: Houston, Circum-Pacific Council for Energy and Mineral Resources, Earth Science Series 1, p. 187–199.

——— 1994, Geologic map of the Klamath Mountains, California and Oregon: U.S. Geological Survey Miscellaneous Investigations Series I-2148, scale 1:500,000, 2 sheets.

——— 2003, Correlation of the Klamath Mountains and Sierra Nevada: U.S. Geological Survey Open-File Report OF 02-0490, 123 p.

Irwin, W. P., and Lipman, P. W., 1962, A regional ultramafic sheet in eastern Klamath Mountains, California, Geological Survey Research: U.S. Geological Survey Professional Paper 450-C, p. C18–C21.

Irwin, W. P., and Mankinen, E. A., 1998, Rotational and accretionary evolution of the Klamath Mountains, California and Oregon, from Devonian to present time: U.S. Geological Survey, Open-File Report 98-114, 1 map sheet.

Irwin, W. P., and Wooden, J. L., 1999, Plutons and accretionary episodes of the Klamath Mountains, California and Oregon: U.S. Geological Survey, Open-File Report 99-374, 1 sheet.

Kelsey, H. M., Engebretson, D. C., Mitchell, C. E., and Ticknor, R. L., 1994, Topographic form of the Coast Ranges of the Cascadia margin in relation to coastal uplift rates and plate subduction: Journal of Geophysical Research-Solid Earth, v. 99(B6), p. 12,245–12,255, doi:10.1029/93JB03236.

Ketcham, R. A., 2005, Forward and inverse modeling of low-temperature thermochronometry data: Reviews in Mineralogy and Geochemistry, v. 58, p. 275–314, doi:10.2138/rmg.2005.58.11.

Ketcham, R. A., Donelick, R. A., and Carlson, W. D., 1999, Variability of apatite fission track annealing kinetics: III. Extrapolation to geological time scales: American Mineralogist, v. 84, p. 1235–1255.

Ketcham, R. A., Donelick, R. A., and Donelick, M. B., 2000, AFTSolve: A program for multi-kinetic modeling of apatite fission-track data: Geological Materials Research, v. 2, n. 1, electronic.

Lanphere, M. A., Irwin, W. P., and Hotz, P. E., 1968, Isotopic age of the Nevadan orogeny and older plutonic and metamorphic events in the Klamath Mountains, California: Geological Society of America Bulletin, v. 79, p. 1027–1052, doi:10.1130/0016-7606(1968)79[1027:IAOTNO]2.0.CO;2.

Lindsley-Griffin, N., Griffin, J. R., and Farmer, J. D., 2006, Paleogeographic links between Yreka Terrane (Klamath Mountains, Northern California) and Alaska's Nixon Fork and Alexander Terranes: Geological Society of America Abstracts with Programs, v. 38, n. 5, p. 36.

MacDonald, D. F., 1910, The Weaverville-Trinity Center gold gravels, Trinity County, California: United States Geological Survey Bulletin, n. 530, p. 48–58.

MacGintie, H. D., 1937, The flora of the Weaverville beds of Trinity County, California; with descriptions of the plant-bearing beds, *in* Eocene flora of western America: Carnegie Institute of Washington Contributions to Paleontology, Publication No. 465, p. 83–151.

McDougall, I., and Harrison, T. M., 1999, Geochronology and thermochronology by the ^{40}Ar/^{39}Ar method: New York, Oxford University Press, 269 p.

Miller, D. S., Duddy, I. R., Green, P. F., Hurford, A. J., and Naeser, C. W., 1985, Results of interlaboratory comparison of fission-track age standards: Fission-track workshop-1984: Nuclear Tracks and Radiation Measurements, 10, p. 381–391, doi:10.1016/0735-245X(85)90127-9.

Mortimer, N., and Coleman, R. G., 1985, A Neogene structural dome in the Klamath Mountains, California and Oregon: Geology, v. 13, p. 253–256, doi:10.1130/0091-7613(1985)13<253:ANSDIT>2.0.CO;2.

Nilsen, T. H., 1984, Tectonics and sedimentation of the Upper Cretaceous Hornbrook Formation, Oregon and California, *in* Crouch, J. K., and Bachman, S. B., editors, Tectonics and sedimentation along the California Margin: Society of Economic Paleontologists and Mineralogists, Pacific Section, Field Trip Guidebook, v. 38, p. 101–117.

Phillips, P. A., ms, 1989, The geology of the Weaverville Formation in the vicinity of Weaverville, California: Arcata, California, Humboldt State University, M.Sc. thesis, 174 p.

Phillips, P. A., and Aalto, K. R., 1989, The Weaverville Formation: implications for tectonically-controlled basin development in the central Klamath Mountains, *in* Colburn, I., Abbott, P., and Minch, J., editors, Conglomerates in basin analysis: Los Angeles, Pacific Section, Society of Economic Paleontologists and Mineralogists, v. 62, p. 81–98.

Saleeby, J. B., Harper, G. D., Snoke, A. W., and Sharp, W. D., 1982, Time relations and structural-stratigraphic patterns in ophiolite accretion, west central Klamath Mountains, California: Journal of Geophysical Research 87(B5), p. 3831–3848, doi:10.1029/JB087iB05p03831.

Schweickert, R. A., and Irwin, W. P., 1989, Extensional faulting in southern Klamath Mountains, California: Tectonics, v. 8, p. 135–149, doi:10.1029/TC008i001p00135.

Snoke, A. W., and Barnes, C. G., 2006, The development of tectonic concepts for the Klamath Mountains province, California and Oregon, *in* Snoke, A. W., and Barnes, C. G., editors, Geological studies in the Klamath Mountains province, California and Oregon: A volume in honor of William P. Irwin: Geological Society of America Special Paper, v. 410, p. 1–29, doi:10.1130/2006.2410(01).

Spencer, J. E., 1984, Role of tectonic denudation in warping and uplift of low-angle normal faults: Geology, v. 12, p. 95–98, doi: 10.1130/0091-7613(1984)12<95:ROTDIW>2.0.CO;2.

Stockli, D. F., Farley, K. A., and Dumitru, T. A., 2000, Calibration of the apatite (U-Th)/He thermochronometer on an exhumed fault block, White Mountains, California: Geology, v. 28, p. 983–986, doi: 10.1130/0091-7613(2000)28<983:COTAHT>2.0.CO;2.

Stone, L., Moley, K., Aalto, K. R., and Renne, P. R., 1993, The Pliocene-Pleistocene sedimentary tectonic history of NW California: Geological Society of America Abstracts with Programs 25:5, p. 151–152.

Wright, J. E., and Fahan, M. R., 1988, An expanded view of Jurassic orogenesis in the western United States cordillera: Middle Jurassic (pre-Nevadan) regional metamorphism and thrust faulting within an active arc environment, Klamath Mountains, California: Geological Society of America Bulletin, v. 100, p. 859–876.